

EFFECT OF LIQUEFACTION OF SOIL FOUNDATION ON INELASTICITY OF UNDERGROUND RC DUCTS

Mohammad Reza OKHOVAT^{*1}, Koichi MAEKAWA^{*2}, Shang FENG^{*3}

ABSTRACT

In this paper, damage of underground RC ducts having interaction with liquefied soil foundations is discussed by using nonlinear dynamic finite element analysis coupled with soil. The simulation is performed in both drained and undrained conditions to clarify the effect of liquefaction on the response of structure. The results show ground liquefaction greatly deteriorates the soil skeleton stiffness and results in the reduced damage to RC structures even though large displacement occurs. It implies that the required ductility of RC ducts can be moderated if the liquefaction risk is high.

Keywords: underground structure, liquefaction, response evaluation, finite element method

1. INTRODUCTION

Less damage to large underground reinforced concrete (RC) ducts was reported compared to on-ground structures although damages to small pipelines were observed as early as 1964 in Niigata Earthquake and Alaska Earthquake [1]. This fact made structural engineers deem that underground RC structures might be rather safe during earthquakes until Hyogoken-Nanbu earthquake in 1995, when severe damages and collapse of RC underground subway stations and ducts were first experienced [2]. Later, this kind of catastrophic damage was repeated again in the earthquake of 1999 Chi-Chi, Taiwan [3]. Therefore, the earthquake-induced damages to large underground RC structures and rational earthquake resistant design have received remarkable attention.

Although the seismic performance of large underground structures has been extensively studied (e.g. [2, 4]), there have been limited researches regarding the liquefaction-related seismic performance of RC structures. Liu and Song [5] investigated the dynamic behaviors of a subway station in liquefiable sand subjected to horizontal and vertical earthquake excitations. Kimura *et al.* [6] conducted some centrifuge model tests to study the effect various countermeasures against liquefaction of sand deposits with an underground structure. In most of these researches, however, the focus was addressed on the behavior of soil itself during seismic motions and the up-lift rigid body motion of buried structures. The present study tries to have deeper views towards the inelastic performance of underground RC structures subjected to earthquake excitations considering the nonlinearity of both structures and soil foundations.

Seismic design actions for underground ducts are generally characterized in terms of forced displacement

and/or mean strains imposed on the structure. The rational and practical approach is to implicitly consider the interaction of underground RC with surrounding grounds. First, free-field ground deformations due to a seismic event are estimated and second, the underground RC is designed to accommodate these deformations through fictitious soil spring. This approach is satisfactory especially when lower levels of shaking are anticipated or the underground facility is in a stiff medium such as rocks [4].

In this paper, inelasticity and damage of RC ducts like subway tunnels, having interaction with liquefiable soils, is targeted. In order to determine the effect of liquefaction on seismic response of structures, both drained and perfectly undrained states of pore water are discussed. Liquefaction may greatly increase in the deformation of soil around structures, but at the same time, the stiffness and internal stress of soil are dramatically reduced, too. A question is raised, what is the resultant of these two mentioned kinematics in RC nonlinearity?

2. NONLINEAR CONSTITUTIVE MODELS

2.1 Constitutive Model for Reinforced Concrete

A reinforced concrete material model has been constructed by combining constitutive laws for cracked concrete and that for reinforcement. The fixed multi-directional smeared crack constitutive equations [7] are used as the relations of spatially averaged stresses and strains. Crack spacing or the density and diameter of reinforcing bars are implicitly taken into account in smeared and joint interface elements no matter how large there are.

The constitutive equations satisfy uniqueness for compression, tension and shear of cracked concrete. The bond performance between concrete and

*1 Ph.D Candidate, Dept. of Civil Engineering, The University of Tokyo, JCI Member

*2 Professor, Dept. of Civil Engineering, The University of Tokyo, JCI Member

*3 Ph.D Candidate, Department of Hydraulic and Hydropower Engineering, Tsinghua University, P. R. China

reinforcing bars is taken into account in terms of tension-stiffness and the space-averaged stress-strain relation of reinforcement is assumed to represent the localized plasticity of steel. The hysteresis rule of reinforcement is formulated based upon Kato's model for a bare bar under reversed cyclic loads. This RC in-plane constitutive modeling has been verified by member-based and structural-oriented experiments. Herein, the authors skip the details of the RC modeling and refer to [8, 9, 10].

2.2 Constitutive Model for Soil

A nonlinear path-dependent constitutive model of soil which can predict the nonlinear response of layered soil under earthquake excitation is essential to simulate the behavior of the entire RC-soil system properly. Here, the multi-yield surface plasticity concept [7] is applied to formulate the stress-strain relationship of the soil following Masing's rule for the shear hysteresis [11]. The authors also use the framework of elasto-plastic and damaging concrete modeling to formulate the soil nonlinearity as follows.

The basic idea of this method is rather simple. First, the total stress applied on soil particle assembly, denoted by σ_{ij} , can be decomposed of deviatoric shear stresses (s_{ij}) and compressive mean pressure (p) as,

$$\sigma_{ij} = s_{ij} + p\delta_{ij} \quad (1)$$

where δ_{ij} is Kronecker's delta symbol.

Soil is idealized as an assembly of finite numbers of elasto-perfectly plastic components, which are conceptually connected in parallel. Each component is given different yield strength, so all components yield at different total shear strains, which results in a gradual internal yielding. Thus, the nonlinear behavior appears naturally as a combined response of all components. Hence, the authors propose the total shear stress carried by soil particles being expressed with regard to an integral of each component stress as,

$$s_{ij} = \sum_{m=1}^n s_{ij}^m(\varepsilon_{kl}, \varepsilon_{kl}^m, G^m, F^m) \quad (2)$$

$$ds_{ij}^m = 2G_0^m de_{ij}^m = 2G_0^m (de_{ij} - de_{pij}^m)$$

$$de_{pij}^m = \frac{s_{ij}^m}{2F^m} df$$

$$df = \frac{s_{kl}^m de_{kl}}{F^m} = \frac{s_{kl}^m d\varepsilon_{kl}}{F^m}$$

where G_0^m is the initial shear stiffness of the m -th component, and F^m is the yield strength of the m -th one. These component parameters can be uniquely decided from the shear stress strain relation [12].

In general, the volumetric components may fluctuate and affect the shear strength and stiffness of soil skeleton. In fact, the shear strength of soil may decay when increasing pore water pressure brings reduced confining stress to soil particle skeletons. The multi-yield surface plastic envelope may inflate or contract according to the confinement stress as shown

in Fig. 1. It can be formulated by summing up the linear relation of the shear strength and the confinement stress as,

$$\begin{aligned} F^m &= \chi F_{ini}^m \quad (3) \\ \chi &= \frac{(c - I_1' \tan \phi)}{S_u} \\ I_1' &= \frac{(\sigma_1' + \sigma_2' + \sigma_3')}{3} \end{aligned}$$

where, F_{ini} is the multi-surface plastic envelope, χ is the confinement index, (c, ϕ) are cohesive stress and frictional angel, and S_u is the maximum shear strength.

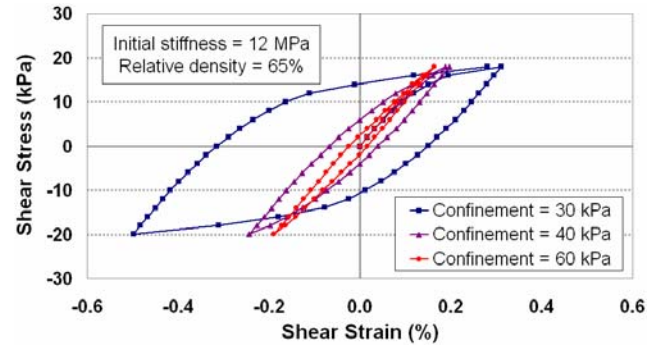


Fig.1 Confinement dependent soil model under drained cyclic shear loading

For simulation of the pore-water pressure and related softening of soil stiffness in shear, the volumetric nonlinearity of soil skeleton has to be taken into account. The authors simply divide the dilatancy into two components according to the microscopic events of soil particles. One is the consolidation or negative dilation as unrecoverable plasticity denoted by ε_{vc} . The other is the positive dilatancy associated with alternate shear stress due to the overriding of soil particles, which is denoted by ε_{vd} as,

$$p = 3K_0(\varepsilon_0 - \varepsilon_v), \quad \varepsilon_v = \varepsilon_{vc} + \varepsilon_{vd} \quad (4)$$

where K_0 is the initial volumetric bulk stiffness of soil particles assembly.

The volumetric irreversible contraction of particle will cause increasing pore pressure under hardly undrained states, which may lead to liquefaction. According to experiments of sandy soils, the following formulae are adopted as,

$$\varepsilon_{vc} = \varepsilon_{v,lim} \left\{ 1 - \exp\left(-2(J_{2p} + J_{2p,ini})\right) \right\} - \varepsilon_{vc,ini} \quad (5)$$

which is represented by the accumulated shear of soil skeleton denoted by J_{2p} [9, 12] and $\varepsilon_{v,lim}$ is the intrinsic volumetric compacting strain corresponding to the minimum void ratio as,

$$\begin{aligned} \varepsilon_{v,lim} &= 0.1(\log_{10} I_1^{0.6} + 1.0) \\ \varepsilon_{vc,ini} &= \varepsilon_{v,lim} \left\{ 1 - \exp(-2J_{2p,ini}) \right\} \end{aligned}$$

If the relative density of soil is assumed to be D_r ,

the following relation can be used to inversely decide $J_{2p,ini}$, which is a constant corresponding to the initial compactness of soil particles as,

$$D_r(\%) = \frac{\varepsilon_{vc,ini}}{\varepsilon_{v,lim}} = \left\{ 1 - \exp(-2J_{2p,ini}) \right\} \quad (6)$$

The shear provoked dilatancy which is path-independent and defined by the updated shear strain intensity denoted by J_{2s} as below.

$$\varepsilon_{vd} = \eta \frac{(aJ_{2s})^2}{1 + (aJ_{2s})^2} \quad (7)$$

$$J_{2s} = \sqrt{\frac{1}{2} e_{ij} e_{ij}}, \quad \eta = \frac{0.015(\varepsilon_{vc} + \varepsilon_{v,ini})}{\varepsilon_{v,lim}}, \quad a = 25.0$$

According to the elasto-plastic and continuum damaging model of concrete [7], equivalent plasticity can be represented in general form with respect to the elastic scalar function as,

$$J_{2p} = \int dJ_{2p}^m, \quad dJ_{2p}^m \equiv \frac{1}{2} \bar{s}_{kl}^m d\varepsilon_{kl} \quad (8)$$

Then, the dilatancy factor can be defined in each component with different plastic range. Within this scheme, the liquefaction induced nonlinearity and cyclic dilatancy evolution can be consistently computed. Fig. 2 shows the pure shear stress-strain relation and the corresponding pore pressure of undrained soil. Shear stiffness decay and cyclic mobility can be seen.

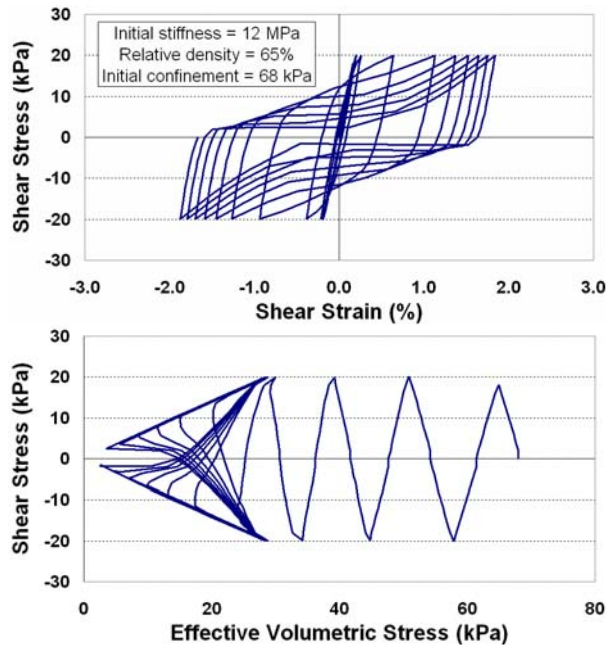


Fig.2 Confinement dependent soil model under undrained cyclic shear loading

2.2 Constitutive Model for Interface between RC and Soil

In this paper, the linear elastic model which assumes a bilinear relation for the opening/closure

mode is employed to model the interfacial kinematics. The normal stress is zero in case of separation, which means no stress is transferred between the soil and the structure when the interface is open. On the other hand, the contact stiffness in closure mode is assigned a large value to ensure that no overlap is allowed, as shown in Fig. 3(a). For shear sliding mode, shear stress–slip relation is assumed to be linear-plasticity as shown in Fig. 3(b). The contact may slide if the applied shear stress exceeds the frictional shear strength, which is assumed to follow the Coulomb law. To apply this model, the initial condition of the soil–structure interface must be simulated to represent the actual static earth pressure. This is achieved by applying the natural gravity action of the soil mass alone before applying the dynamic action of the base rock [7, 12].

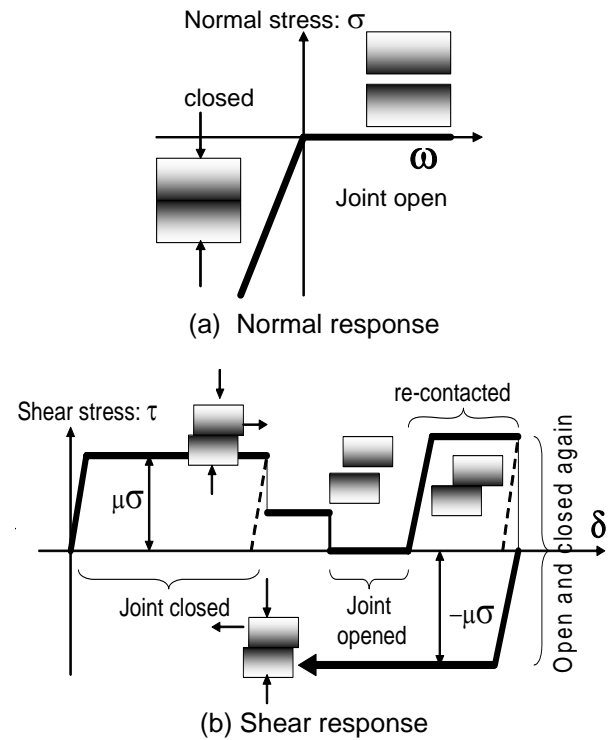


Fig.3 Normal and shear response of linear elastic interface model [13]

3. FINITE ELEMENT MODEL

3.1 Model Properties

To investigate the seismic behaviors of underground RC ducts, a typical subway tunnel section is modeled whose wall and slab dimensions are shown in Fig. 4. The center column to mainly support the dead weight of soil overlay has a rectangular cross section of 0.60×0.80 m and is idealized as firmly fixed to the slabs. The clear distance between two adjacent columns along the line is 3 m. The tunnel is stiffened with 45° haunches at the corners and has a longitudinal reinforcement ratio of 1.1% for side walls and slabs, 1.6% for the column, and web reinforcement ratio of 0.2% for all elements. Compressive strength of concrete and yield strength of steel are 24 MPa and 240

MPa, respectively.

The soil deposit is assumed to be loose sand with a thickness of 15 m which is located on a 5-meter-thick layer of non-liquefiable soil which again lies on the bedrock as shown in Fig. 4. The detail of material property for non-liquefiable soil layer is shown in Table 1.

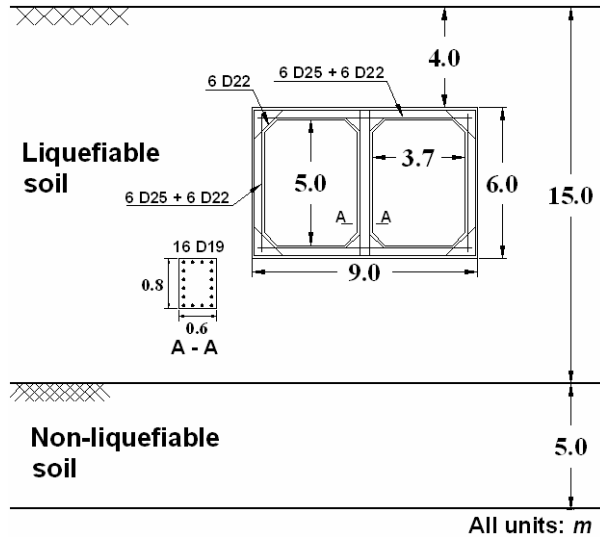


Fig.4 Soil-structure system geometry

Table 1 Material property for non-liquefiable layer

Initial shear stiffness	105 MPa
SPT <i>N</i> -value	15
Dry unit weight	16 kN/m ³
Friction angle	40 °
Cohesion	100 kPa
Relative Density	75%

By assuming the plane strain condition, the finite element mesh used in the analysis is composed of eight-node isoparametric two-dimensional elements for both RC and soils. The RC-soil interfacial elements are placed at an interface in between the soil and the RC elements. Since the angle of internal friction of the model sand is 30°, the friction angle of the interface is obtained using the relation $\delta = \tan^{-1}[(2/3) \tan \phi]$, which is about 21°. Totally, 7303 nodes and 2352 elements are arranged in the dynamic model. The north-south component of the rock base acceleration measured at 1995 Kobe earthquake, which is scale-adjusted to 0.3g based on the measurement at Kobe meteorological observatory, is used as the input bed rock motion in the seismic analysis. It shows a high horizontal ground acceleration with a short period as shown in Fig. 5.

The overall experimental verification of the interaction analysis with soil and RC ducts was reported in [14].

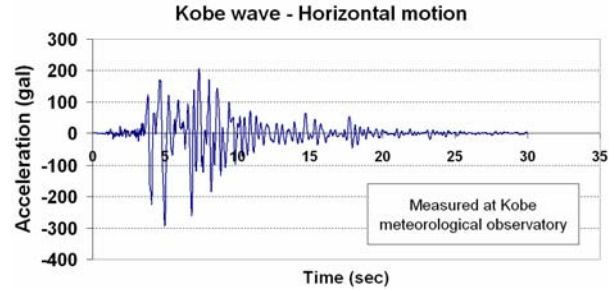


Fig.5 Input earthquake motion

3.2 Boundary Conditions

The boundary between the soil deposit and the bedrock is simply assumed to be fixed and would act as the bottom boundary of the analyzed domain at which the earthquake motion is imposed. The ground surface is assumed to be flat and free of loadings and the underground water level is assumed to locate up to the ground surface level when the soil is saturated.

The seismic behavior of the soil deposit in the far fields of the underground structure should assume the response of a free field. In the shaking table tests of soil-structures, a laminar shear box may be used to simulate the quasi-far-field boundary [15]. Here, quasi-far-field elements with a length of 10 m are placed at each extreme side of the analysis domain. The stiffness and unit weight of these elements are increased 100 times with respect to adjacent soil elements of the domain. As the far-field mode of seismic motion is simple shear, the length of the boundary condition (about the half of the domain height) is selected so that the bending deformation mode would not occur. In addition, confinement independent soil elements are used in the quasi-far-field zone in order to prevent the edge collapse in analysis. This boundary allows the harmonized horizontal and vertical displacements similar to the case of laminar shear box.

Several trial analyses were conducted to determine the size of the analyzed domain. Finally, a relative large analyzed domain (200 m) is used to make the reflected wave too weak to affect the calculated response in the focal part of interest to the authors.

3.3 Analytical Approach

The seismic analyses of the soil-structure system require that an initial stress field in equilibrium be obtained beforehand [5, 7]. Therefore, an initial static drained analysis was firstly performed to determine the initial stress field and static earth pressure on the duct. This static stress field is then used as the initial condition for the subsequent dynamic run with the input excitation. The geological and construction history or path-dependence of the soil-structure system is not perfectly considered. But, the authors consider that this initial stress states may not be serious because so large inelastic plasticity is induced to the soil under greatly large ground motions.

In order to investigate the effect of soil liquefaction on the damage of underground RC ducts, several models with and without the ducts are analyzed

in both drained and undrained states of pore water with various initial stiffness (G_0) which is increased from 12 MPa to 230 MPa as shown in Table 2. The structure is assumed to be located inside the soil at a depth of 4 m without any change in the mesh property of the remaining soil elements.

Table 2 Material property for first soil layer

SPT N -value	G_0 (MPa)	Relative Density (%)
1	12	25
3	29	28
5	44	32
10	76	40
15	105	48
20	132	56
25	158	65
30	182	75
40	230	80

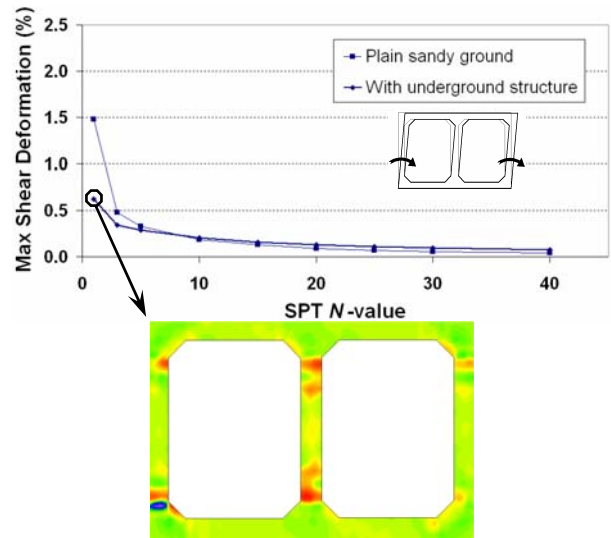
It should be pointed out that a fully undrained condition is assumed for saturated soil elements during the seismic action which could be an extreme case but still a reasonably clear assumption, because the required time for drainage of a several-meter-thick sand layer is 10-30 min which is much longer than the duration time of earthquake loading [15].

4. NUMERICAL RESULTS

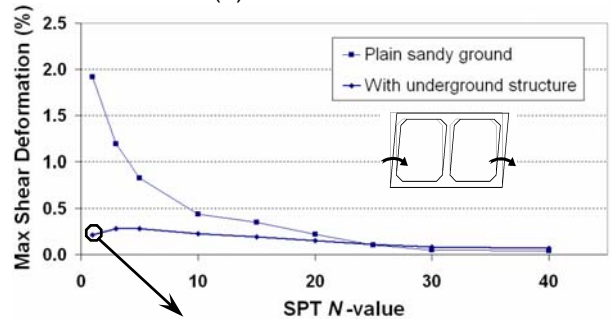
Fig. 6 shows the maximum shear deformation response spectrum of the RC duct and the soil volume which replaces it in the plain sandy grounds. It can be observed that the on-going practical design approach based on the free-field ground deformations can well predict the deformational demand on the underground RC structures in somehow stiffer soil mediums. In soft layers of soil which consists of loosely deposited sand, however, the design based on the free-field ground deformations would result in overestimated deformational demand on the structural members as shown in Fig. 6(a).

Besides, liquefaction may significantly bring about increased soil deformation which indicates that large soil strains with associated large degradation of the shear stiffness have developed within the ground. Hence, the underground RC duct which is located in the regions where the underground water level is high and designed without considering the interaction with the surrounding ground results in large amount of web reinforcement or large dimensions of structural elements for ductility demand.

However, because of the deterioration of the surrounding soil stiffness which takes place in liquefied soil, the deformation demand on the RC duct would dramatically decrease resulting in less damage to the tunnel as shown in Fig. 6(b). Therefore, that large amount of reinforcement or thick structural elements is not necessary.



Strain state of tunnel at maximum shear deformation (a) Drained condition



Strain state of tunnel at maximum shear deformation (b) Undrained condition

Fig.6 Effect of soil stiffness on shear deformation

Fig. 7 shows the up-lift displacement of the duct in both saturated and unsaturated loose sand ($N_{spt}=5$). It can be understood that the duct would have some settlement during the ground motions in drained condition, while liquefied soil would push the underground duct upward significantly as it was observed in the past earthquakes [15]. Therefore, some countermeasures should be considered to reduce the uplift of underground structure in liquefiable soils.

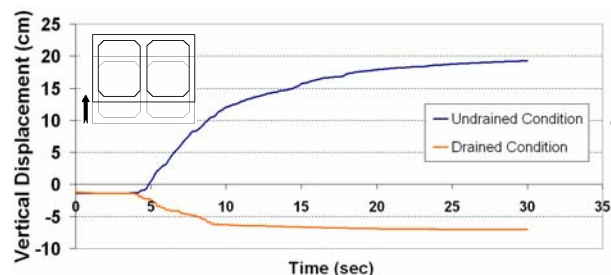


Fig.7 Vertical displacement of the tunnel

The excess pore pressure responses of the saturated sandy layer with and without RC, at the centerline of the domain and 2.5 m below the structure are shown in Fig. 8. The excess pore pressures are expressed in terms of the ratio of excess pore pressure to the initial effective overburden pressure. It can be seen that the degree of liquefaction below the duct is lower with the presence of duct. In fact, the flotation of the underground lightweight structure would cause larger shear deformation of soil which contributes to the lowering of excess pore pressure. This is reasonable for most medium loose and medium dense sand, since in larger shear deformation, the sand tends to dilate, which shall lead to the lowering of excess pore pressure if it is saturated [5].

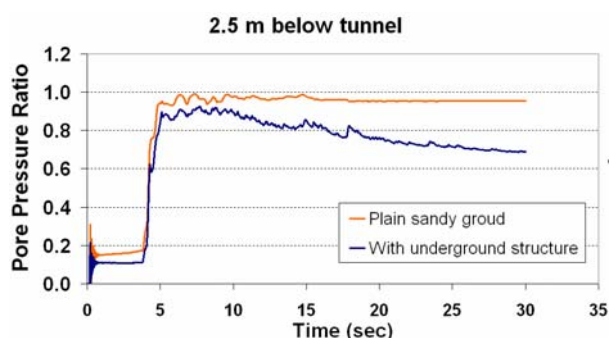


Fig.8 Excess pore pressure in soil

5. CONCLUSIONS

In soft layers of soil which consists of loosely deposited sand, the design based on the large free-field ground deformations would result in high deformation demand on the structural elements which in turn requires large amount of reinforcement or large dimensions of structural elements. This situation would become even more severe in the regions where the underground water level is high because liquefaction may occur, which significantly increases the ground deformations.

However, liquefaction would deteriorate the surrounding soil stiffness and thus the deformation demand on the tunnel would consequently decrease. Considering this issue could lead to a more optimum, economical and rational design of the RC underground structures. Finally, it should be pointed out that other countermeasures like sheet piling or increasing the weight of tunnels should be considered to reduce the uplift of underground structure in liquefiable soils.

REFERENCES

[1] W. J. Hall and T. D. O'Rourke: "Seismic Behavior and Vulnerability of Pipelines," Proc. Third US Conf. Lifeline Earthquake Engineering, pp.761-73, 1991.
 [2] A. Shawky and K. Maekawa: "Collapse Mechanism of Underground RC Structures during

Hanshin Great Earthquake," Proc., First Int. Conf. on Concrete Structures, pp.1-17, Egypt, 1996.
 [3] W. L. Wang, T. T. Wang, J. J. Su, C. H. Lin, C. R. Seng and T. H. Huang: "Assessment of Damage in Mountain Tunnels due to the Taiwan Chi-Chi Earthquake," Tunneling Underground Space Technology, Vol. 16, No. 3, pp.133-50, 2001.
 [4] Y. M. A. Hashash, J. J. Hook, B. Schmidt and J. Yao: "Seismic Design and Analysis of Underground Structures," Tunneling Underground Space Technology, Vol. 16, No. 4, pp.247-93, 2001.
 [5] H. Liu and E. Song: "Seismic Response of Large Underground Structures in Liquefiable Soils Subjected to Horizontal and Vertical Earthquake Excitations," Computer Geotechnics, Vol. 32, No. 4, pp.223-44, 2005.
 [6] T. Kimura, J. Takemura, A. Hiro-oka and M. Okamura: "Countermeasures against Liquefaction of Sand Deposits with Structures," Proc. First Int. Conf. on Earthquake Geotechnical Engineering, pp.1203-1224, Tokyo, Japan, 1995.
 [7] K. Maekawa, P. Pimanmas and H. Okamura: "Nonlinear Mechanics of Reinforced Concrete," Spon Press, 2003.
 [8] K. Maekawa and X. An: "Shear Failure and Ductility of RC Columns after Yielding of Main Reinforcement," Engineering Fracture Mechanics, Vol. 65, pp.335-68, 2000.
 [9] K. Maekawa, P. Irawan and H. Okamura: "Path-dependent Three-Dimensional Constitutive Laws of Reinforced Concrete: Formulation and Experimental Verifications," Structural Engineering and Mechanics, Vol. 5, No. 6, pp.743-54, 1997.
 [10] B. Kato: "Mechanical Properties of Steel under Load Cycles Idealizing Seismic Action," CEB Bulletin D'Information, Vol.131, pp.7-27, 1979.
 [11] G. Masing: "Eigenspannungen und Verfestigung Beim Messing," Proc. of Second Int. Congress of Applied Mechanics, p.332, Zurich, 1926.
 [12] T. Maki, K. Maekawa and H. Mutsuyoshi: "RC Pile-Soil Interaction Analysis using a 3D-Finite Element Method with Fiber Theory-based Beam Elements," Earthquake Engineering Structural Dynamics, Vol. 99, pp.1-26, 2005.
 [13] K. Maekawa, N. Fukuura, and M. Soltani: "Path-Dependent High Cycle Fatigue Modeling of Joint Interfaces in Structural Concrete," Journal of Advanced Concrete Technology, Vol.6, No.1, pp.227-242, February 2008.
 [14] Japan Society of Civil Engineers, "Recommended Code and Manual for Seismic Performance Verification of Out-door Important Structures of Nuclear Power Plants," Concrete Library, 2002.
 [15] I. Towhata: "Geotechnical Earthquake Engineering," Springer, 2008.